Front. Phys. China (2006) 4: 424－427
DOI 10.1007/s11467-006-0052-6

RESEARCH ARTICLE

**YANG Xue-feng, WU Fang, SHAN Xu, YAN Mi, WANG Ke-dong,
XUE Xin-xia, CHEN Xiang-jun, XU Ke-zun**

# Electron momentum spectroscopy of the highest occupied molecular orbitals of chlorobromomethane

**Abstract** The first measurement of the complete valence shell binding energy spectra of chlorobromomethane ($CH_2BrCl$) is reported by (e, 2e) electron momentum spectrometer using symmetric non-coplanar geometry at an impact energy of 1200 eV plus binding energy. The experimental electron momentum profiles of the highest occupied molecular orbitals (HOMOs) are extracted and compared with Hartree-Fock (HF) and density functional theory (DFT) calculations. DFT calculation employing B3LYP hybrid functional and the large-sized basis sets provides the best agreement with the experiment.

**Keywords** (e, 2e) electron momentum spectroscopy, symmetric non-coplanar geometry, Hartree-Fock method, density functional theory

**PACS numbers** 34.80.Gs

## 1 Introduction

Chlorobromomethane ($CH_2BrCl$), one of biogenic halocarbons, is a component of microalgae emission in the Atlantic Ocean [1]. Like other halocarbons, it plays an important role in the atmosphere and contributes to powerful ozone-depletion potentials. Therefore, it has received considerable attention and has been investigated extensively by photoelectron spectra (PES) [2－4] using He I, He II and synchrotron radiation light sources, Penning ionization electron spectra (PIES) [3] using He*($2^3S$) metastable atoms and photodissociation dynamics [5] using laser pulses. To our best knowledge, no electron momentum spectroscopy measurement on $CH_2BrCl$ has been reported so far. Therefore, it is necessary and significant to carry out EMS study at the level of orbital wave function for further understanding chemical properties, reaction activity and the ozone- depletion mechanism of the $CH_2BrCl$ molecule.

Electron momentum spectroscopy (EMS) has a unique advantage in exploring the electronic structure of matter [6]. It can not only obtain the ionization energy spectra of atoms and molecules, but also the energy-selected orbital electron density distribution in momentum space, which is the modulus square of orbital wave function. By the comparison of experimental and theoretical momentum distributions, EMS offers a powerful proof for evaluating the quality of various quantum chemical calculations.

## 2 Experimental background

EMS is based on kinematically complete electron collision single-ionization process in which an electron from target atoms or molecules is clearly knocked out by a high- energy incident electron and the residual ion acts as a spectator. Usually, the plane wave impulse approximation (PWIA) can describe the experiment well.

Within the PWIA, as well as target Hartree-Fock (HF) approximation, the (e, 2e) differential cross-section can be described as [6－9]:

$$\sigma_{\text{EMS}} = \text{constant} \times \int \mathrm{d}\Omega_p \left| \varphi_i^{\text{HF}}(\boldsymbol{p}) \right|^2 \tag{1}$$

or in Kohn-Sham (KS) approximation, the (e, 2e) differential cross-section is given by [10－13]:

---

YANG Xue-feng, WU Fang, SHAN Xu, YAN Mi, WANG Ke-dong, XUE Xin-xia, CHEN Xiang-jun, XU Ke-zun
Hefei National Laboratory for Physical Sciences at Microscale, Modern Physics Department, University of Science and Technology of China, Hefei 230026, China
E-mail: xjun@ustc.edu.cn

*Received September 13, 2006*

$$\sigma_{\mathrm{EMS}} = \mathrm{constant} \times \int \mathrm{d}\Omega_p \left| \varphi_i^{\mathrm{KS}}(\boldsymbol{p}) \right|^2 \qquad (2)$$

where $\varphi_i^{\mathrm{HF}}(\boldsymbol{p})$, $\varphi_i^{\mathrm{KS}}(\boldsymbol{p})$ is the momentum space one-electron canonical HF or KS wave function for the *i*th orbital from which the electron ejected.

In this work, the symmetric non-coplanar kinematics is employed in the experiment. Gas phase target molecule is ionized by an impact with a high-energy electron beam ($E_0$ = 1200 eV + binding energy, $I_0 \approx 10\ \mu$A). The scattered and ejected electrons have essentially equal energy and enter into their respective hemispherical energy analyzer along the same polar angles ($\theta_1 = \theta_2 = 45°$). Their relative azimuthal angle $\phi$ is variable over a wide range (0° ~ ± 30°) by rotating one analyzer around the incident electron beam and keeping the other one fixed. By detecting two outgoing electrons in coincidence, the ionization energy spectra are measured at a series of different azimuthal angles, and the electron momentum distributions for individual orbitals are extracted by the deconvolving of a series of ionization energy spectra. The detailed description of the present (e, 2e) spectrometer has been given elsewhere [14]. In this work, the instrumental energy resolution is about 1.3 eV (FWHM) and angular resolution is $\Delta\theta = \pm 1.3^{\circ}$, $\Delta\phi = \pm 1.5^{\circ}$ determined by measuring Ar 3p ionization.

The $CH_2BrCl$ sample with 99.6 % purity was degassed by repeated freeze-pump-thaw cycles, and was used for the present work. No impurities were observed in any of the spectra.

## 3 Results and discussions

$CH_2BrCl$ molecule contains 60 electrons and has $C_S$ point group symmetry. Its ground electronic configuration can be written as:

$$(\mathrm{core})^{40}\ \underbrace{(1a')^2(2a')^2}_{\text{inner valence}}$$

$$\underbrace{(3a')^2(1a'')^2(4a')^2(5a')^2(2a'')^2(6a')^2(7a')^2(3a'')^2}_{\text{outer valence}}$$

The ordering of valence orbitals is adopted from the PES of Tian *et al.* [3]. Figure 1 shows one of the ionization energy spectra of $CH_2BrCl$ over the energy range from 5 eV to 30 eV measured at azimuthal angles $\phi = 7°$ by EMS. Gaussian peaks fitted to the individual transitions are shown by dotted curves while their sum is shown by a solid curve. The positions of each Gaussian peak are estimated according to the ionization potentials from high-resolution PES [2, 4], and the widths are the combinations of EMS instrumental energy resolution (1.3 eV in this work) and Frank-Condon width of the corresponding bands determined by high-resolution PES [2, 4]. Small adjustments in the deconvolution process have been applied to compensate the asymmetries of the shapes of the Franck-Condon profiles. As shown in Fig.1, Gaussian peaks labeled by vertical bars 1—8 are corresponding to the ionizations from 3a''+7a', 6a'+2a'', 5a', 4a', 1a'', 3a', 2a' and 1*a*' orbitals, respectively. Table 1 lists the ionization potentials of the HOMOs from the present EMS and outer valence Green function (OVGF) calculation, together with the previous results from high-resolution PES [2, 3] and OVGF calculation of Tian *et al.* [3].

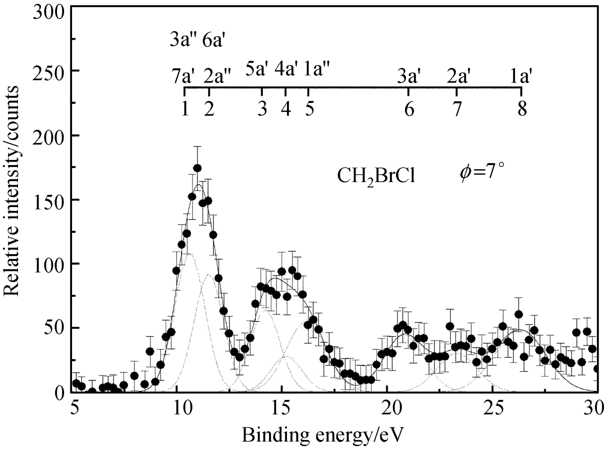

**Fig.1** Binding energy spectra of $CH_2BrCl$ at an azimuthal angle of $\phi = 7°$.

Figure 2 shows the experimental momentum profiles (XMPs) of 3a''+7a', 6a'+2a'' and the summed 4 together with the corresponding calculated results. The theoretical momentum profiles (TMPs) are calculated in the GUASSIAN 98W program [15] using HF and DFT methods with 6-31G, 6-311++G** and Aug-cc-pVTZ basis sets. For the sake of

**Table 1** Ionization potentials for the HOMOs of $CH_2BrCl^a$.

| Experimental | | | Theoretical$^b$ | |
|---|---|---|---|---|
| He I/He II[2,4] | He I[3] | present EMS | OVGF[3]c | present OVGF$^d$ |
| 7a' (10.77) | 3a'' (10.75) | 3a'' (10.87) | 3a'' (10.62)[0.94] | 3a'' (10.73)[0.92] |
| 3a'' (11.06) | 7a' (11.08) | 7a' (10.87) | 7a' (10.65)[0.94] | 7a' (10.73)[0.92] |
| 2a'' (11.81) | 6a' (11.79) | 6a' (11.78) | 6a' (11.43)[0.92] | 2a'' (11.49)[0.92] |
| 6a' (11.81) | 2a'' (11.79) | 2a'' (11.78) | 2a'' (11.50)[0.92] | 6a' (11.59)[0.92] |

$^a$ Ionization potentials are listed in parentheses (in eV); $^b$ Pole strengths in square brackets; $^c$ Basis set: 6-311+G (*d*, *p*); $^d$ Basis set: 6-311 ++$G^{**}$.

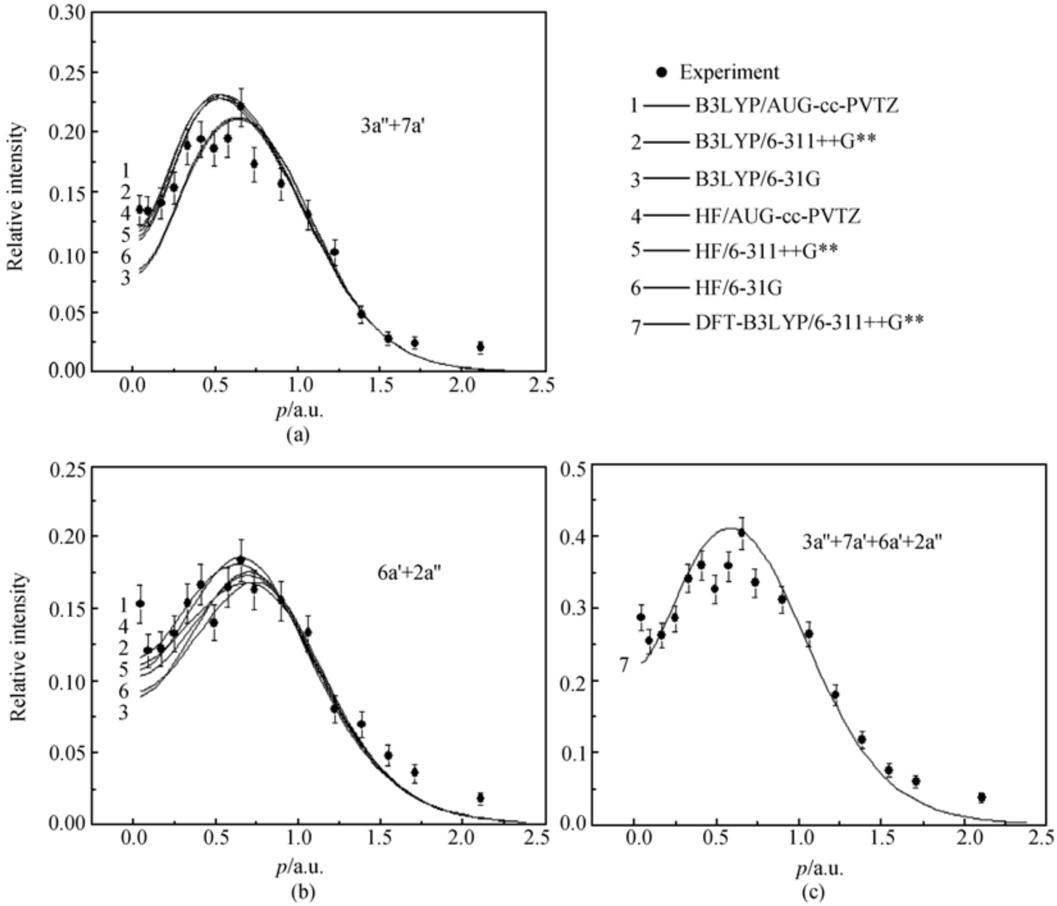

**Fig. 2** Experimental and theoretical momentum profiles for **(a)** 3a"+7a', **(b)** 6a'+2a", **(c)** 3a"+7a'+6a'+2a" of $CH_2BrCl$.

comparison, the instrumental angular resolution was folded into the TMPs using the Gaussian-weighted planar grid method [16]. Moreover, the XMPs and the TMPs are placed on a common intensity scale by normalizing the XMPs of the summed 4 HOMOs (3a"+7a'+6a'+2a") to the corresponding TMPs calculated using B3LYP/Aug-cc-pVTZ.

The HOMOs 3a", 7a' and 6a', 2a" of $CH_2BrCl$ belong to the contributions of Br and Cl lone-pair electrons, respectively. It can be seen from Fig.2 that the XMPs and TMPs of 3a"+7a' and 6a'+2a" all display the expected p-type character. For 3a"+7a', as shown in Fig.2 (a), whether HF or DFT methods, the calculations using 6-31G basis set underestimate the experiment but those using 6-311++G** and AUG-cc-pVTZ basis sets reproduce the experiment well and almost give the same results. It indicates that 6-311++G** basis set has approached saturation and a larger basis set will not be needed. On the other hand, for the same basis sets, HF and DFT calculations show little difference. This suggests that the improvement of calculated results for 3a"+7a' is not dependent on the theoretical method, but depends on the level of the chosen basis set.

For 6a'+2a", as shown in Fig.2 (b), for the same basis sets, DFT-B3LYP calculation is better than HF in accordance with the experiment, indicating that electron correlation effect needs to be considered in the calculation. Generally, the calculations using DFT-B3LYP with larger basis sets 6-311++G** and AUG-cc-pVTZ are in good agreement with the experiment. Figure 2 (c) shows the XMPs of 3a"+7a'+6a'+2a" and compared with the TMPs calculated using DFT-B3LYP with 6-311++G** basis set, a good agreement between the XMPs and TMPs has been achieved.

**Acknowledgements** This work was supported by the National Natural Science Foundation of China (Grant No.10134010).

## References

1. McGivern W. S., Li R. J., Zou P., and North S. W., Photodissociation dynamics of $CH_2BrCl$ studied using resonance enhanced multiphoton ionization (REMPI) with time-of-flight mass spectrometry, J. Chem Phys., 1999, 111: 5771
2. Novak I., Cvitas T., Klasinc L., and Gusten H., Photoelectron Spectra of some Halogenomethanes, J. Chem. Soc., Faraday Trans. II, 1981, 77: 2 049
3. Tian S. X., Naoki K., and Koichi O., Spin-Orbit Coupling Effect and

Intramolecular Orbital Interactions: Penning Ionization of $CH_2BrCl$, $CHBrCl_2$, and $CH_2BrCN$ by Collision with He*($2^3S$) Metastable Atoms, J .Phys. Chem. A, 2003, 107: 2137

4. Novak I. and Benson J. M., UV angle-resolved photoelectron spectra of mixed methylene dihalides using synchrotron radiation, Chem. Phys., 1986, 107: 129
5. Lee S. H., Jung Y. J., and Jung K. H., Photodissociation dynamics of $CH_2BrCl$ at 234 nm. Chemical Physics, 2000, 260: 143
6. McCarthy I. E. and Weigold E., Electron momentum Spectroscopy, Phys. Rep., 1976, 27: 275
7. Brion C. E., Looking at orbitals in the laboratory: the experimental investigation of molecular wavefunctions and binding energies by electron momentum spectroscopy, Int. J. Quantum Chem. ,1986, 29: 1397
8. Coplan M. A. and Moore J. H., Doering J P. (e, 2e) Spectroscopy, Rev. Mod. Phys., 1994, 66: 985
9. Weigold E. and McCarthy I. E., Electron Momentum Spectroscopy, Kluwer-Academic, New York, 1999
10. Duffy P., Chong D. P., Casida M. E., and Salahub D. R., Assessment of Kohn-Sham density-functional orbtials as approximate Dyson orbitals for the calculation of electron-momentum-spectroscopy scattering, Phys. Rev. A ,1994, 50: 4707
11. Casida M. E., Generalization of the optimized-effective-potential model to include electron correlation: A variational derivation of the Sham-Schlüter equation for the exact exchange-correlation potential, Phys. Rev. A, 1995, 51: 2005
12. Duffy P., Calculation of electron momentum distributions using density functional theory, Can. J. Phys., 1996, 74: 763
13. Kohn W. and Sham. L. J., Self-Consistent Equation Including Exchange and Correlation Effects, Phys. Rev. A, 1965, 140: 1133
14. Yang B. X., Chen X. J., Pang W. N., Chen M. H., Zhang F., Tian B. L., and Xu K. Z., Development of (e ,2e) Electron momentum spectrometer and measurement of electron momentum spectrum of Several Atoms and Molecules, Acta. Phys. Sin., 1997, 5: 862 (in Chinese)
15. Frisch M. J., Trucks G. W., and Schlegel H. B. et al., Gaussian 98 Revision A3, Gaussian Inc. Pittsburgh PA, 1998
16. Duffy P., Casida M. E., Brion C. E., and Chong D. P., Assessment of Gaussian-weighted angular resolution functions in the comparison of quantum-mechanically calculated electron momentum distributions with experiment, Chem. Phys., 1992, 159: 347